ANALYSIS AND TESTING OF A METALLIC REPAIR APPLICABLE TO PRESSURIZED COMPOSITE AIRCRAFT STRUCTURE

Adam Przekop
Analytical Mechanics Associates, Inc., Hampton, VA 23666

and

Dawn C. Jegley, Marshall Rouse, Andrew E. Lovejoy
NASA Langley Research Center, Hampton, VA 23681

ABSTRACT

Development of repair technology is vital to the long-term application of new structural concepts on aircraft structure. The design, analysis, and testing of a repair concept applicable to a stiffened composite panel based on the Pultruded Rod Stitched Efficient Unitized Structure was recently completed. The damage scenario considered was a mid-bay to mid-bay saw-cut with a severed stiffener, flange, and skin. A bolted metallic repair was selected so that it could be easily applied in the operational environment. The present work describes results obtained from tension and pressure panel tests conducted to validate both the repair concept and finite element analysis techniques used in the design effort. Simulation and experimental strain and displacement results show good correlation, indicating that the finite element modeling techniques applied in the effort are an appropriate compromise between required fidelity and computational effort. Static tests under tension and pressure loadings proved that the proposed repair concept is capable of sustaining load levels that are higher than those resulting from the current working stress allowables. Furthermore, the pressure repair panel was subjected to 55,000 pressure load cycles to verify that the design can withstand a life cycle representative for a transport category aircraft. These findings enable upward revision of the stress allowables that had been kept at an overly-conservative level due to concerns associated with repairability of the panels. This conclusion enables more weight efficient structural designs utilizing the composite concept under investigation.

1. INTRODUCTION

This section contains a brief description of the Environmentally Responsible Aviation (ERA) project under which the work described in this paper was conducted. Next, the Pultruded Rod Stitched Efficient Unitized Structure (PRSEUS) is introduced as the primary structural concept being explored within the ERA project. Finally, a specific challenge stemming from the repairability of PRSEUS panels is outlined as a motivation for this work.

1.1 Environmentally Responsible Aviation Project

Created in 2009 as part of NASA's Aeronautics Research Mission Directorate's Integrated Systems Research Program, the ERA Project explores and documents the feasibility, benefits and technical risk of vehicle concepts and enabling technologies to reduce aviation's impact on the environment. ERA's Airframe Technology subproject aims to reduce aircraft weight by 10%.

1.2 Pultruded Rod Stitched Efficient Unitized Structure

The primary structural concept being pursued as an important component of next generation airframe technology under the ERA Project is the PRSEUS [1-4], illustrated in Figure 1. This concept is being developed in a partnership between NASA and The Boeing Company for application to future transport aircraft with the goal of developing lighter structure so that the aircraft will require less fuel and produce fewer pollutants. The PRSEUS structure is highly-integrated, weight-efficient, and has damage-arresting capabilities. In this concept a stitched carbon-epoxy material system is used. By stitching through the thickness of a dry material system, the labor associated with panel fabrication and assembly can be significantly reduced. When stitching through the thickness of pre-stacked skin, stringers and frames, the need for mechanical fasteners is almost eliminated. In addition, stitching reduces delamination and improves damage tolerance, allowing for a lighter structure with more gradual failures than traditional composites without through-the-thickness reinforcement.

The PRSEUS concept consists of carbon-epoxy panels fabricated from dry components stitched together, after which the resin is infused in an oven while the panel is subjected to vacuum pressure. Skins, flanges and webs are composed of layers of carbon material that are pre-kitted into multi-ply stacks. A single stack has a thickness of 1.32 mm (0.052 in.) and comprises seven plies with stacking sequence $[+45, -45, 0, 90, 0, -45, +45]_T$ where the percentage of the 0-, 45- and 90-degree fibers are equal to 44.9, 42.9 and 12.2, respectively. Several pre-kitted stacks are used to build up the desired thickness and configuration. Stiffener flanges are stitched to the skin using Vectran thread, and no mechanical fasteners are used for joining. To maintain the panel geometry during fabrication, first stiffeners and then the skin are placed in a tool for stitching prior to moving the assembly to a curing tool for consolidation in the oven. The stiffeners running in the axial direction consist of webs with unidirectional carbon fiber rods at the top of the web. The stack material forming the stiffener web also overwraps the rod to form the stiffener cap. The stiffeners in the lateral direction are foam-filled hats. The manufacturing process is described in detail in ref. [3]. In the current study the frames are 0.508 m (20 in.) apart and stringers are 0.152 m (6 in.) apart. The frames are 0.152 m (6 in.) tall and the stringers are 0.038 m (1.49 in.) tall.

While providing unique advantages in weight, damage tolerance and manufacturing, the PRSEUS concept also presents some inherent challenges not shared by conventional metallic airframes. Among these challenges is the need for design concepts for manufacturing joints and repair techniques for rod-stiffened panels. While both manufactured joints and repairs must be light-weight and meet design load requirements, they are typically applied in different environments. While in a factory environment, a large component with extensive damage might be replaced in its entirety. However, in the operational environment the replacement of a large highly-integrated component with localized damage is often cost-inefficient and impractical. In addition, composite technology-based repair such as bonding requires a tightly controlled environment, perishable supplies, highly skilled workers and advanced tooling to produce a reliable bond. This may be acceptable in a factory environment, but may not be feasible in the field. Since, from a practical standpoint, basic repairs cannot depend on the availability of a factory-like environment, repair techniques applicable to PRSEUS panels in an operational environment were developed [5, 6].

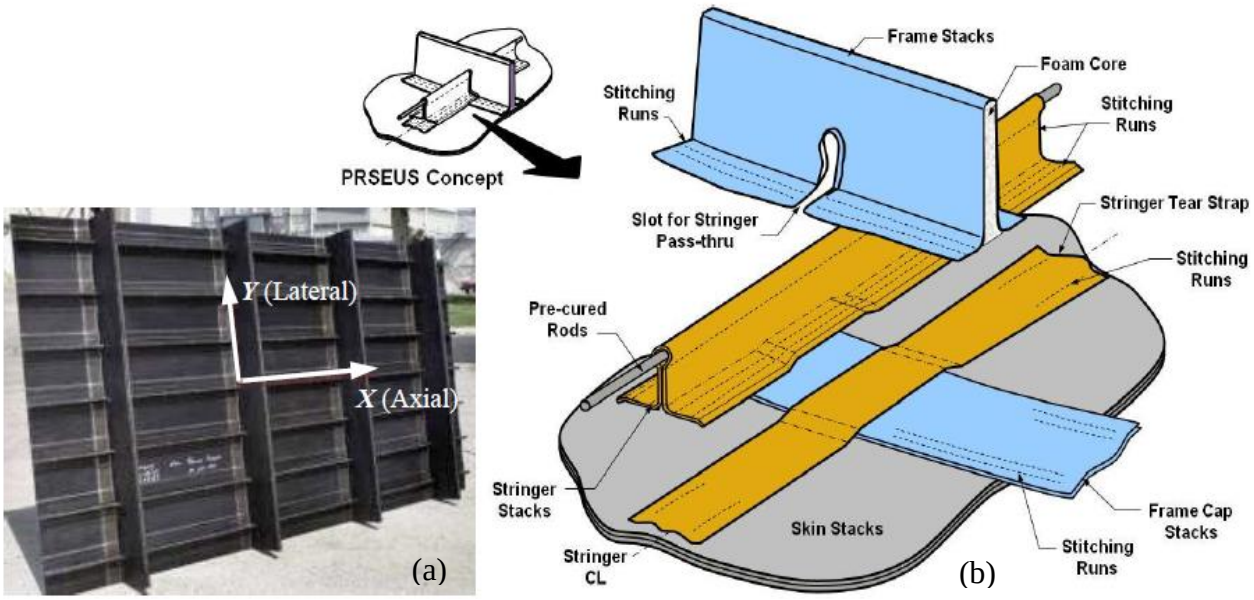

Figure 1. PRSEUS: (a) sample panel and (b) exploded view of the assembly.

1.3 Tension Repair Allowable as a Limiting Design Metric

Based on previous experience, tension loading was designated as a critical design condition [3, 4]. As a result, repairability of PRSEUS panels was regarded as a possible limiting factor in panel design. Consequently, a conservative value of 379 MPa (55 ksi) working stress allowable was routinely applied in preliminary vehicle-level sizing efforts [3,4]. The repair design effort described herein assumed a more aggressive 414 MPa (60 ksi) working stress allowable to challenge this limitation. In other words, a successful repair design sustaining 414 MPa stress allowable could enable further mass savings in the primary airframe structure.

2. METALLIC REPAIR CONCEPT

This section describes the general bolted metallic repair concept. A specific design originally developed for a tension-loaded three-stringer PRSEUS panel is introduced along with a brief summary of the related validation testing [5, 6].

2.1 Tension Panel Repair Design

First and foremost, the repair assembly was required to restore the original load carrying capability of the pristine panel while incurring the smallest weight penalty possible. In general, while not formulated as a quantitative metric, the mechanical behavior and load paths of the repaired panel resembling that of the pristine panel were also required. In addition, established design practices such as those regarding spacing requirements between metallic fasteners applied to a composite primary structure were followed. Finally, operational factors, e.g. what is practical in the environment that the repair technique is intended to be applied, also influenced the design.

The general repair concept was first proposed by The Boeing Company and its initial exploration was conducted in proprietary studies using simplified models and small test articles. The overall configuration of the repair as applied to a three-stringer tension panel is illustrated in Figure 2. Additional details pertaining to titanium fastener sizes and stiffened side repair details are

provided in Figure 3. The repair assembly consists of two aluminum alloy stiffened side pieces (also referred to as angles) whose bottom surfaces rest on the center stringer flange surface and the vertical portions are parallel to the stringer web and surround the pultruded rod. These two stiffened side pieces are riveted together above the rod. The clearance between the two pieces and the pultruded rod ensures that the repair is not clamped on the rod. The flange sections of the repair components are bolted through the panel flanges to an aluminum alloy smooth side strap (also referred to as a doubler). The width of this strap extends to both sides such that its edges can be bolted to the flanges of both outside stringers.

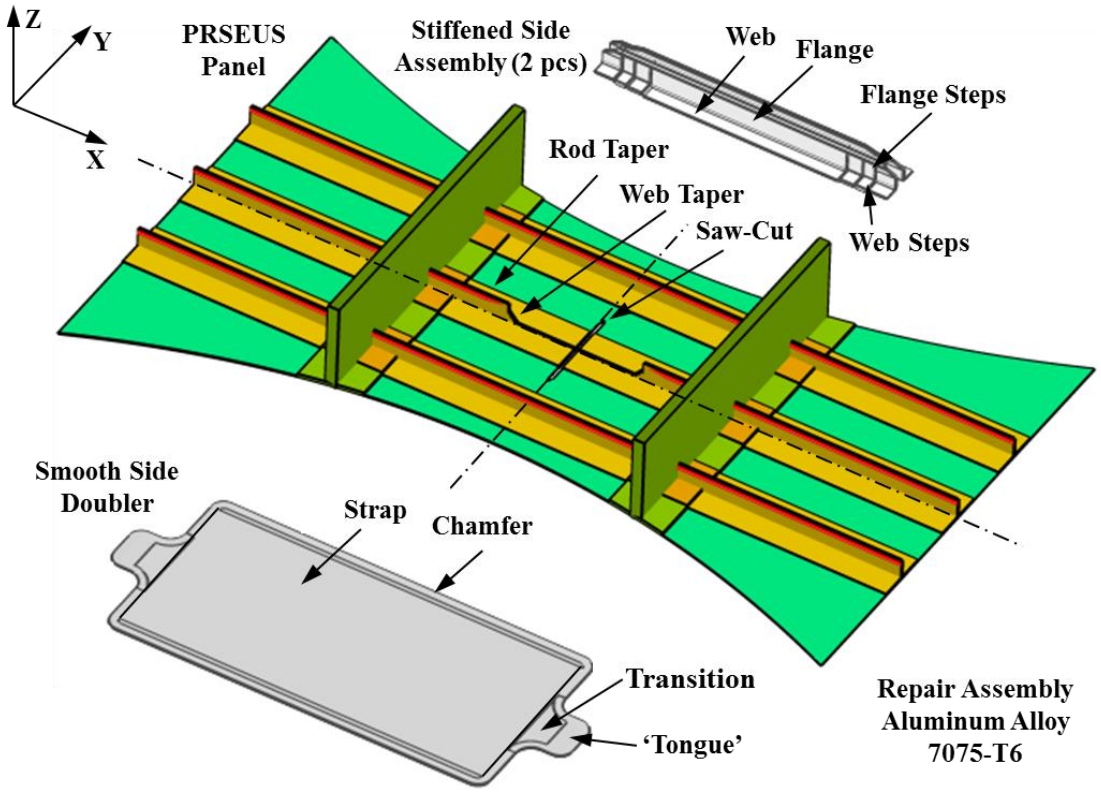

Figure 2. Exploded view of the bolted metallic assembly and the tension repair panel.

Note, that by incorporating a stiff pultruded rod offset from the panel surface, the pristine PRSEUS panels are designed to efficiently carry not only in-plane, but also bending loads. Consequently, the repair concept is designed such that the neutral bending axis of the general cross-section of the three assembled repair pieces (the two stiffened side pieces and the smooth side doubler) coincides with the neutral bending axis of the pristine panel in its general cross-section. This way the repair assembly can transfer combined in-plane and bending loads in a similar fashion as the pristine panel.

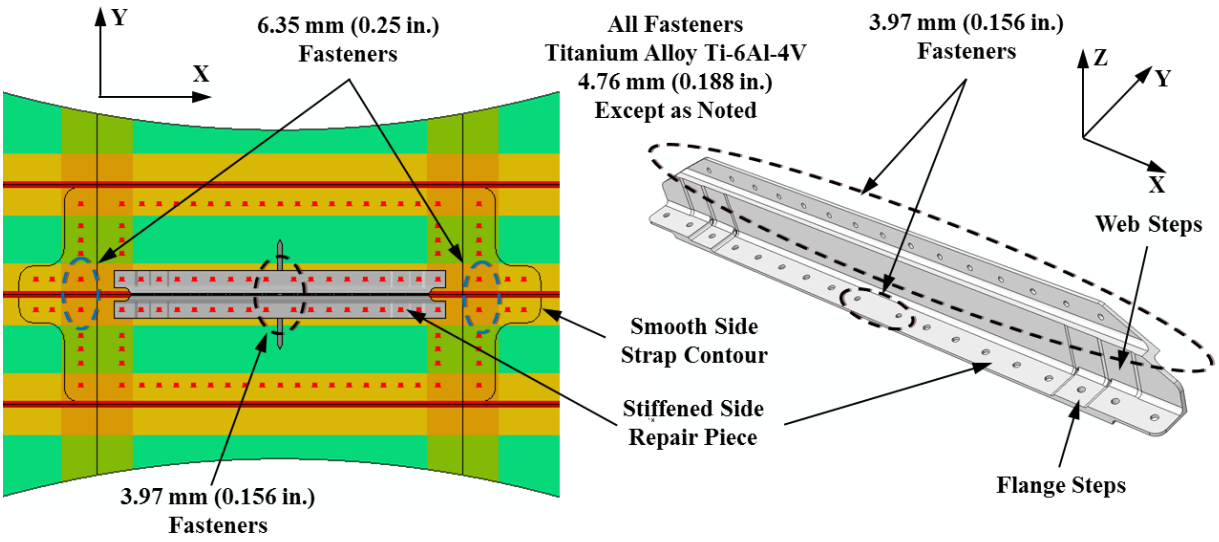

Figure 3. Stiffened side metallic assembly and fastener pattern details.

Finally, note that the taper of the center stringer is not considered a part of the damage but rather it is a part of the repair design. The repair design requires that loads from the severed stringer be transferred into the repair assembly, yet the stringer web thickness of only 2.64 mm (0.104 in.) renders bolted attachment through the webs impractical due to very limited bearing surface. Thus, as part of the repair design, the center web and rod are machined such that the loads from the center stringer are diverted into the flange where they can be gradually transferred to the repair by fasteners through the flange.

2.2 Tension Panel Testing Summary

The panel was tested at the NASA Langley Research Center (LaRC) in the one million pound load-rated test machine. The test was conducted at room temperature. The tension load was applied through displacement-control and was introduced at the rate of 1.27 mm (0.05 in.) per minute. The final panel failure occurred at the loading of 1,085 kN (244,000 lbf). After applying a statistical scatter knock-down factor of 15%, this load corresponds to the working stress allowable of 480 MPa (69.6 ksi). Recall from section 1.3 that this exceeds not only the previous working stress allowable, but also the design objective of 414 MPa (60 ksi). The failure mode is illustrated in Figure 4. The failure occurred away from the center section of the panel, i.e., away from the initial saw-cut damage, generally in the vicinity of the top foam-filled frame.

Very good correlation of the finite element (FE) analysis and test results was obtained up to the tension design limit load (DLL). Above that level the comparison was still favorable but plasticity in the metallic repair assembly combined with a simplified fastener modeling began to show detrimental effects on the correlation of the results. A detailed discussion of the test and analysis results is presented in ref. [6].

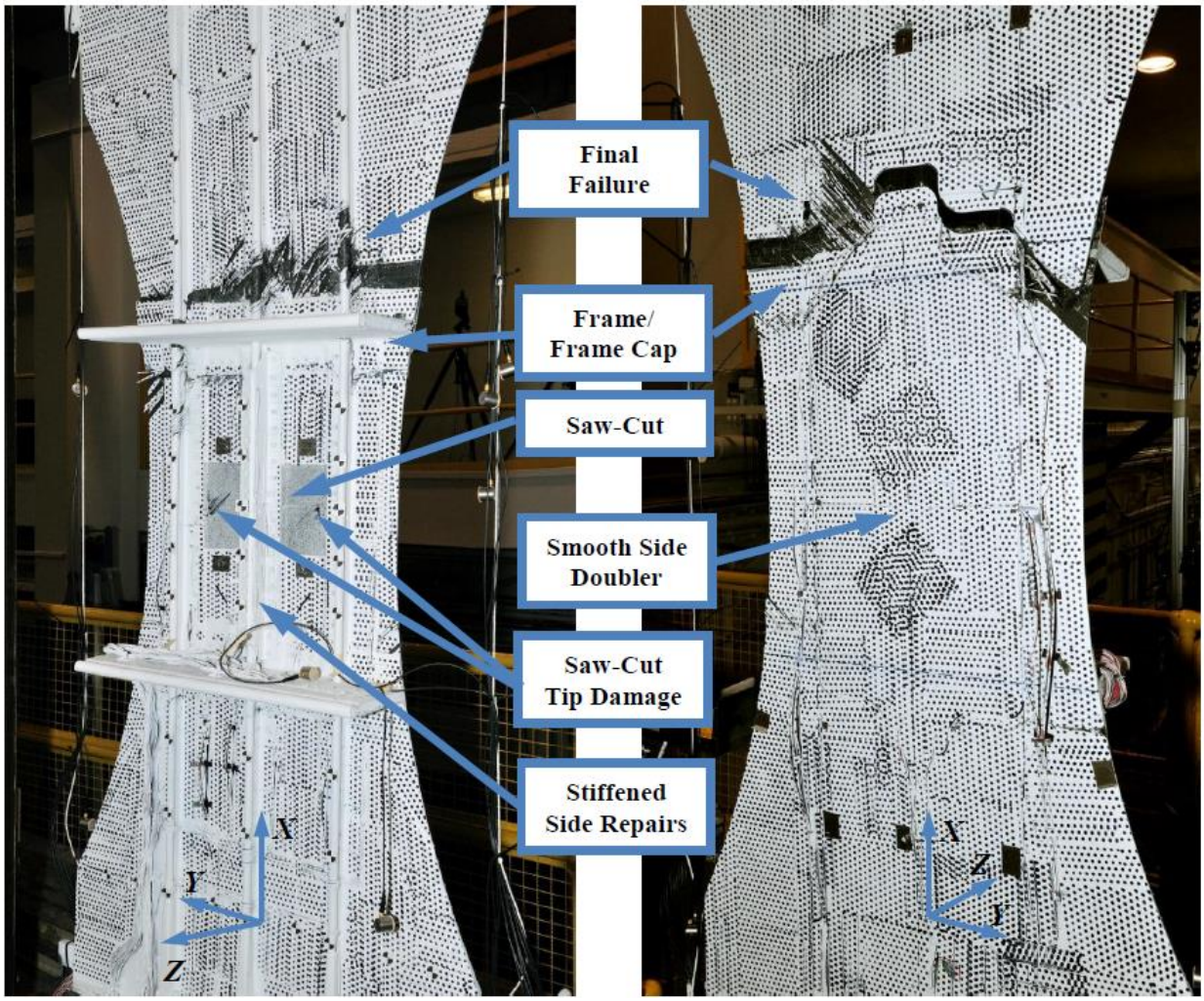

Figure 4. Repaired tension panel failure away from the saw-cut damage.

3. REPAIR PRESSURE PANEL STATIC NONLINEAR FINITE ELEMENT ANALYSIS AND TESTING

This section describes the PRSEUS pressure panel loaded in its pristine condition and subsequently after a barely visible impact damage (BVID) was applied. In the latter condition the panel was tested until failure occurred in a non-catastrophic fashion. Such a failure enabled repair and further testing, i.e., the main scope of this work. The repaired panel configuration, its instrumentation and testing are described in this section. FE modeling is also discussed and the results from the predictive nonlinear analysis are correlated with the test data.

3.1 Pressure Panel Test Article

The pristine pressure panel installed on a steel pressure vessel is shown in Figure 5. The outer dimensions of the panel were 2.74 m by 1.22 m (108 in. by 48 in.). The opening in the top of the pressure vessel was 2.54 m by 1.02 m (100 in. by 40 in.) so that a width of 0.102 m (4 in.) around the perimeter of the panel was clamped. It is seen in Figure 5 that the installation fixture

additionally extended toward the center of the panel over the two frame caps (in the X-direction) and 15 stringer flanges (in the Y-direction). The stiffened side of the panel before installation to the pressure vessel is shown in Figure 6, where the aforementioned frame caps and stringer flanges are visible. Stiffener geometry and spacing are the same as for the tension panel. Material properties of the panel and metallic repair installed after the panel sustained damage in the initial testing are listed in Table 1.

Table 1. Material properties of the PRSEUS panel and repair assembly.

Material	**E_1, GPa (Msi)**	**E_2, GPa (Msi)**	**ν_{12}**	**G_{12}, GPa (Msi)**
Rod, Toray T800/3900-2B	111 (16.1)		0.30	42.7 (6.19)
Stack Properties, AS4-VRM34	67.2 (9.74)	33.5 (4.86)	0.40	16.3 (2.37)
Foam Core, Rohacell 110WF	0.145 (0.021)	0.145 (0.021)	0.32	0.055 (0.008)
Aluminum Alloy 7075-T6	71.0 (10.3)	71.0 (10.3)	0.33	26.7 (3.87)
Titanium Alloy Ti-6Al-4V Grade 5	114 (16.5)	114 (16.5)	0.342	44.0 (6.38)

The panel was initially tested in its pristine condition up to 126.86 kPa (18.4 psi), considered the design ultimate load (DUL). No identifiable damage occurred during this test. Subsequently, the stiffening rod of the first off-center stringer and the skin section between this stringer and the center stringer were impacted with an energy level resulting in BVID [7]. After impact, the pressure panel was again tested up to the DUL without any signs of additional damage. Next, the pressure load was increased until failure, which occurred in a non-catastrophic fashion at 193 kPa (28 psi). The panel retained its pressurization capability and the pressure was further increased to 207 kPa (30 psi). After the test the only visible damage identified was in the center stringer (i.e., not the impacted stringer), slightly off its mid-span location. The stiffening rod of the stringer was compression-crushed and the stringer's web exhibited damage as shown in Figure 7. The extent and location of the damage presented an opportunity to reuse the panel for testing in a repaired configuration. Note, that the damage of the center stringer occurred within its section that would be tapered off before repair installation, as shown on the tension panel in Figure 2. Therefore, after tapering the center stringer and introducing the same 0.152 m (6 in.) long by 6.35 mm (0.25 in.) wide mid-bay to mid-bay saw-cut, the three metallic repair components identical to those described in section 2.1 were installed on the panel. The smooth side of the repair panel with the doubler is shown in Figure 8 and the two metallic angles installed on the stiffened side of the panel are shown in Figure 9. The inset in Figure 9 shows the tapered stringer before the two repair angles were installed.

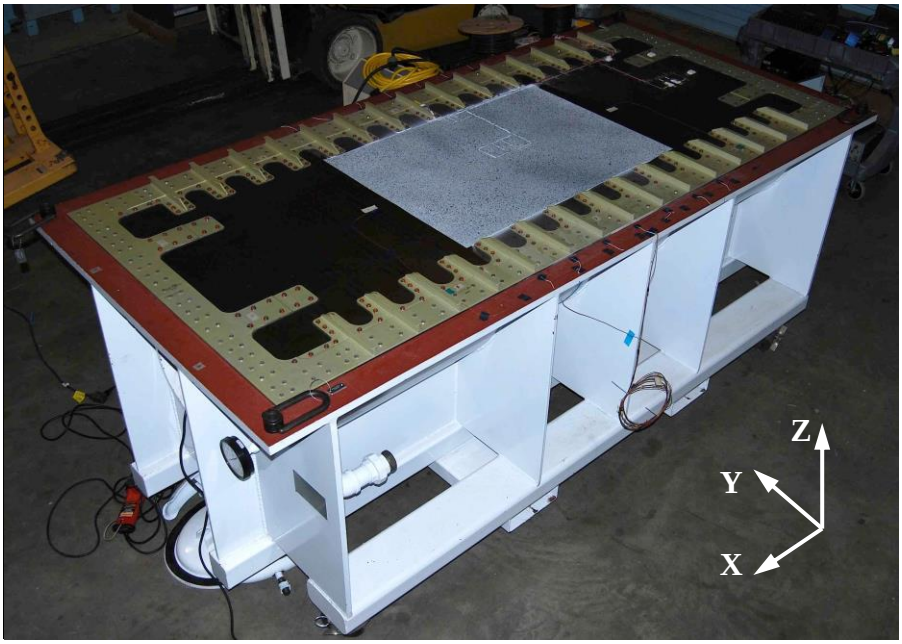

Figure 5. Pressure vessel with the pristine test panel installed.

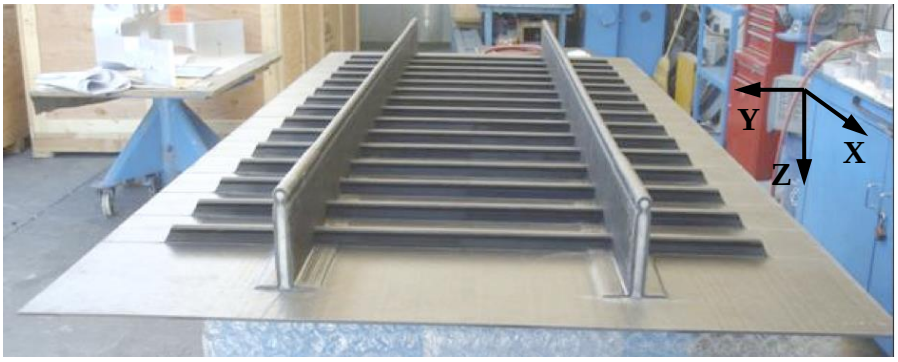

Figure 6. Stiffened side of the pressure panel before installation onto the pressure vessel.

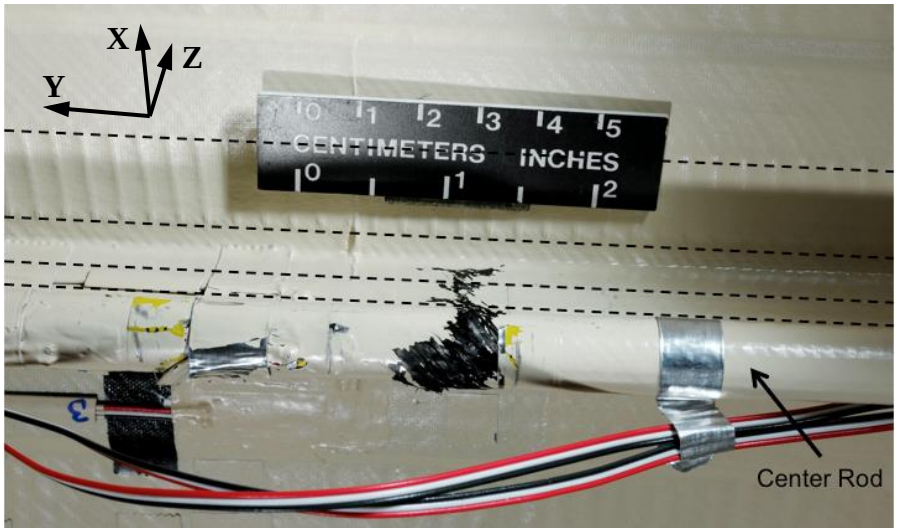

Figure 7. Crushing failure of the center stringer. The dashed lines identify stitch locations.

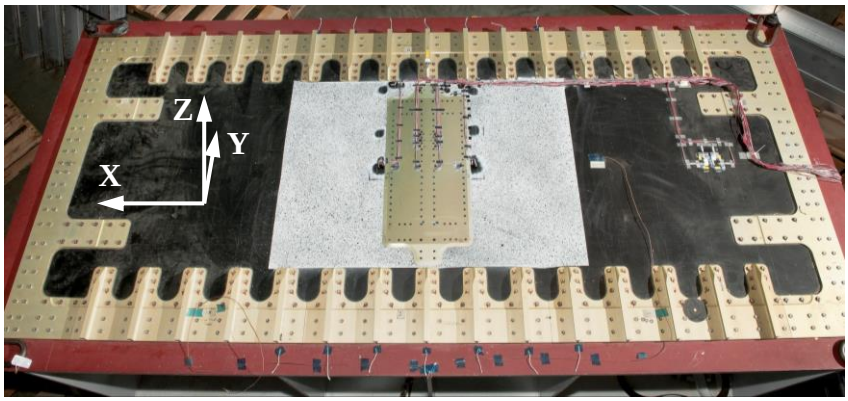

Figure 8. Repaired panel with the smooth side doubler installed.

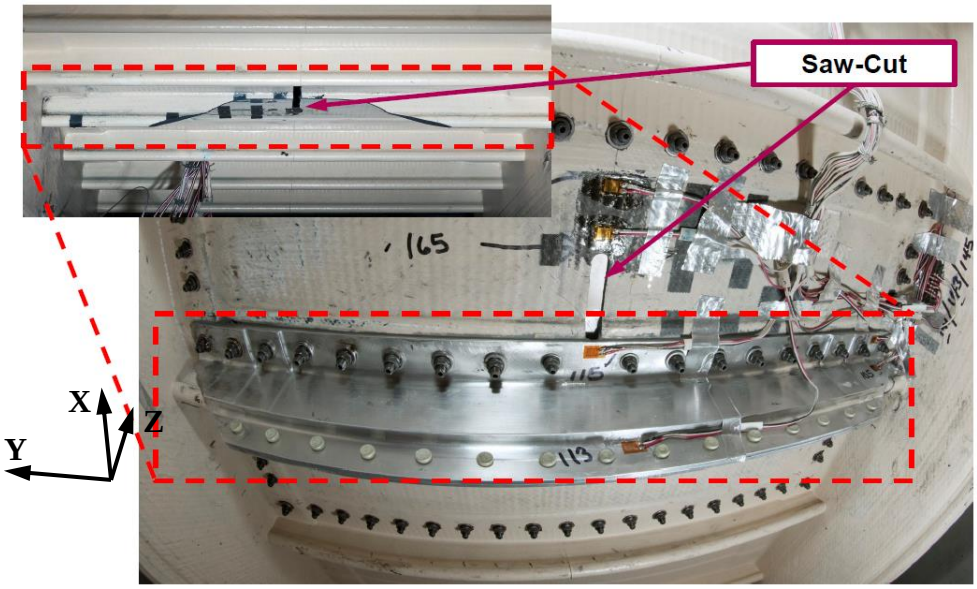

Figure 9. Stiffened side of the repaired panel with the two aluminum angles installed.

Most of the strain gages originally installed for the pristine and BVID testing [7] were retained on the repaired panel as long as they did not interfere with the repair installation, as they would provide data for comparison between pristine and repaired panel responses. Additional gages were added on and near the repair assembly. The complete pattern of 50 strain gages is not presented here for brevity. Section 3.3 contains plots that illustrate only locations of the gages used in the discussion of the results. Additionally, a video image correlation in three-dimensions (VIC-3D) technique [8] was used on the outside center section of the repaired test article. Figures 5 and 8 show the 1.02 m by 0.737 m (40 in. by 29 in.) speckle pattern area used in the VIC-3D measurements for the pristine and BVID testing. Once the outer doubler was installed, as presented in Figure 8, the same section was painted with a similar speckle pattern.

3.2 Finite Element Modeling and Analysis

The commercial FE package NASTRAN [9] was used in the analysis effort. The pressure panel model comprised shell and beam elements. The repair assembly was modeled using shell elements only. The typical element size for the panel and repair was 5 to 6 mm (0.20 – 0.24 in.).

To accurately represent the boundary conditions of the panel, a model of the pressure vessel was also created using shell elements. Discretization of the pressure vessel was much coarser with an approximate element size of 50.8 mm (2 in.). The panel was connected to the pressure vessel using connector elements placed at the bolt locations. The same modeling technique was used to attach the repair assembly to the panel. The number of elements in the model approached 140,000, resulting in approximately 840,000 degrees-of-freedom. Nonlinear static analysis (solution 106) was conducted to obtain pre-test predictions.

3.3 Test and Predictive Analysis Results Correlation

The repaired panel test was conducted in the Combined Loads Test System (COLTS) facility located at NASA LaRC. Pressure was applied at a quasi-static rate of approximately 10.3 kPa (1.5 psi) per minute in the room temperature environment. The final pressure of 207 kPa (30 psi) was achieved without any visible damage. VIC-3D and strain data were recorded at 1 Hz sampling rate.

The VIC-3D out-of-plane displacement fields acquired in the center section of the panel described in section 3.1 were compared with the corresponding FE analysis results. Comparisons conducted at the DLL of 63.43 kPa (9.2 psi), DUL of 126.86 kPa (18.4 psi), and DUL+10% of 139.55 kPa (20.24 psi) resulted in very similar quality agreement. Therefore, only the DUL case is shown in Figure 11. The top section of the plot presents the entire VIC-3D speckle pattern area. The bottom section presents the solution for the entire FE model and the corresponding area is indicated with a dashed line. The maximum displacement occurs in skin sections away from the panel center since the center of the panel is stiffened by the repair. Overall, the qualitative shape comparison is very good and the maximum displacement from the analysis exceeds the measurement by only 6%.

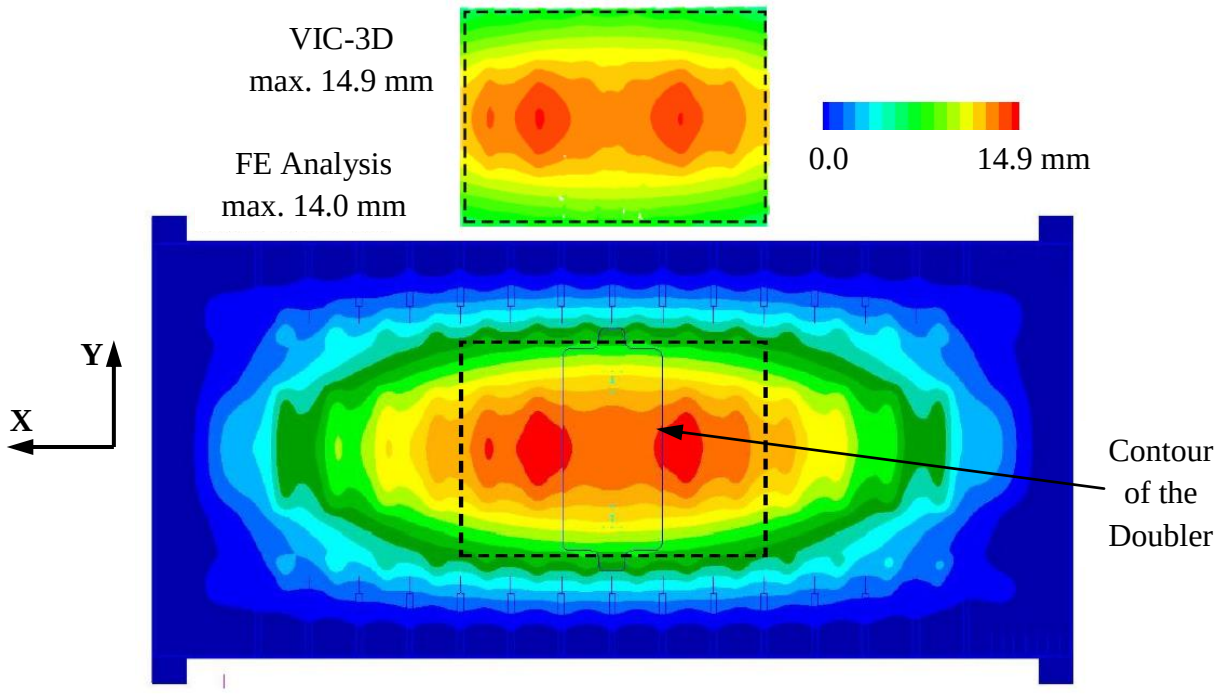

Figure 11. Out-of-plane displacement at DUL of 126.86 kPa (18.4 psi).

Results obtained at selected gage locations are presented next to assess strain correlations obtained in distinct sections of the repaired panel. Specifically, results obtained on the composite panel are shown in Figure 12, on the repair doubler in Figure 13, and on the repair angles in Figure 14. In each plot the test results are shown as solid lines as the pressure was increased, while the FE results are shown as the same color circles only at the three pressure levels introduced at the beginning of this section. All the comparisons are generally favorable. In the composite panel (Figure 12) strains measured in the X-direction by the red and blue curves are captured very accurately by the analysis, and transition from a slight compression below approximately the DLL of 63.43 kPa to a slight tension above this level. Strains in the Y-direction by the black and green curves exhibit nearly linear behavior in tension. The analysis accurately captures the linear trend but tends to slightly under-predict the strain values.

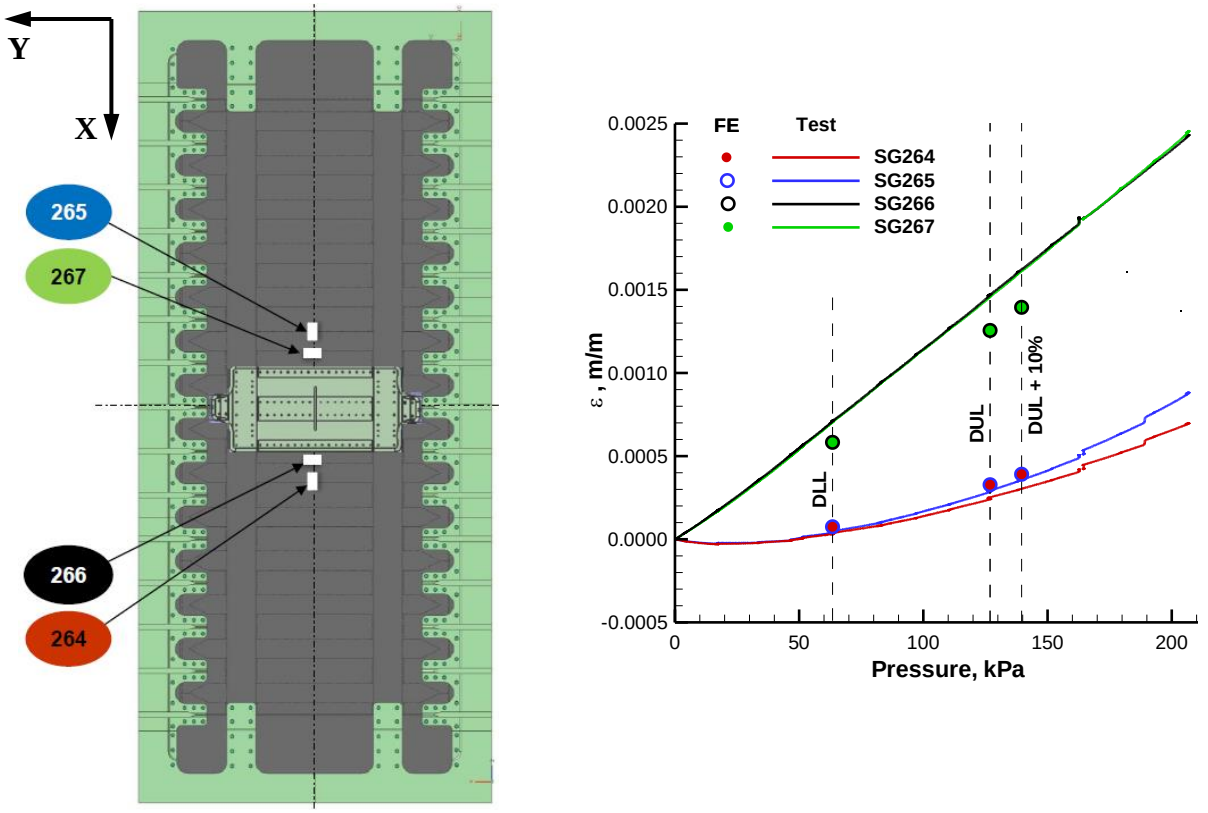

Figure 12. Strains on the smooth side of the composite panel near the doubler.

Strains measured near the center of the doubler (Figure 13) also show linear characteristics and the trend is accurately captured by the analysis, although again the analysis tends to under-predict the measurements. Note that the analysis assumes a symmetric test article while the measured data is not exactly symmetric. Both doubler edge gages show slight nonlinearities in measurements that are not captured in the analysis. Since slight discontinuities are visible in the measured data, a settling of the repair is suspected and it may be amplified by single-shear fasteners as no inner repair components extend to those locations. The settling appears to be more pronounced on one side of the strap that the other.

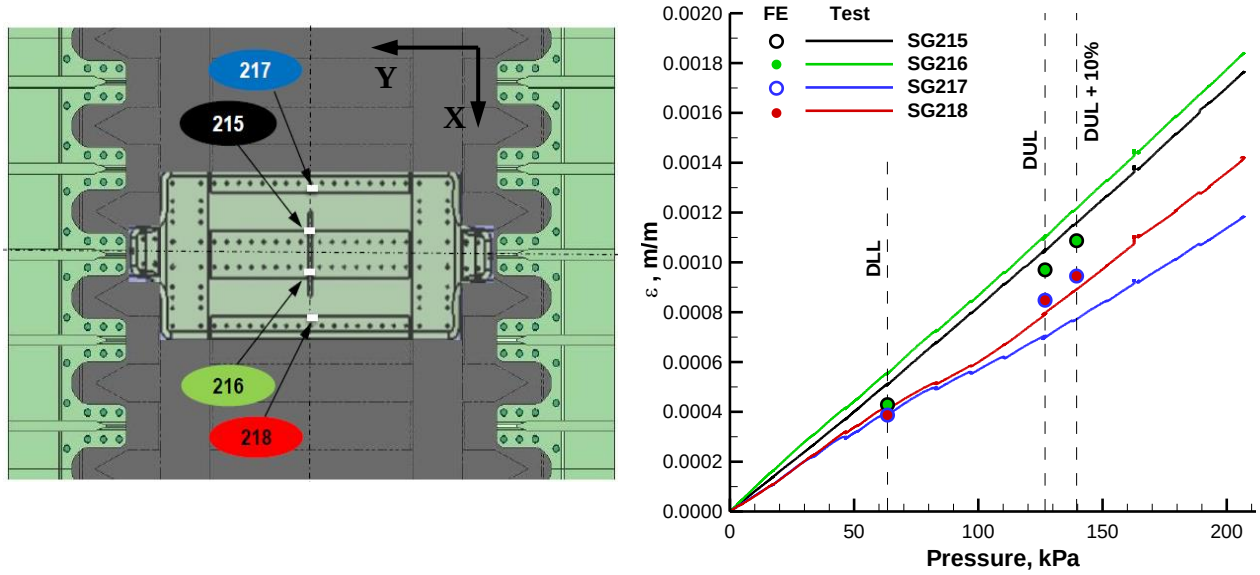

Figure 13. Strains in the repair doubler.

Finally, the strains on the inner repair angle are compared in Figure 14. Since this location is dominated by bending in the positive Z-direction, strains in the repair flange are in tension as shown by the black curve, and strains at the tip of the angle's web are in compression, as shown by the blue curve. The two measurements are captured accurately by the analysis, however, the tension is slightly under-predicted and compression is slightly over-predicted. This combination may be indicative of the fact that the actual neutral bending axis in the panel was located further away from the panel surface than in the FE model. Note that installation imperfections, such as a liquid shim applied between the repaired stringer flange and the repair's angle flange, were not considered in the FE model. This shim thickness might contribute to the neutral bending axis misalignment between the test article and the FE model.

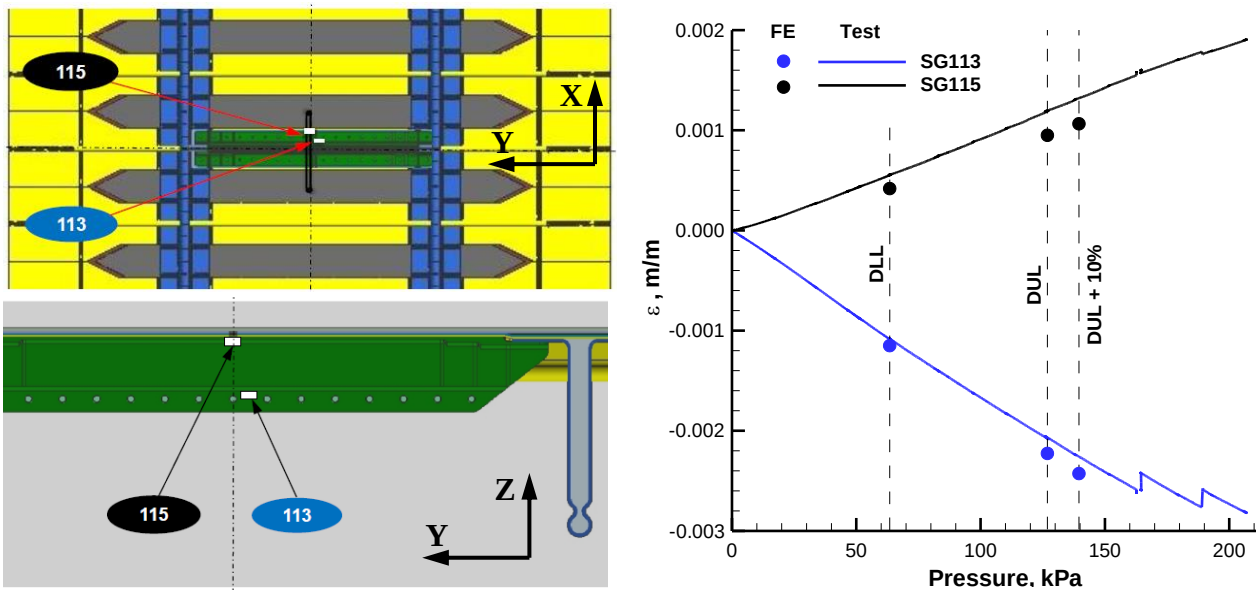

Figure 14. Strains in the repair angle.

4. LOW-CYCLE FATIGUE TESTING

While several static tests of PRSEUS panels have been conducted in a building-block approach [1-4, 6, 7], the only cyclic loading tests were performed on single-frame and single-stringer specimens under mechanical compression [10]. No pressure testing representative of an airframe low-cycle fatigue was performed thus far. The repair panel's withstanding the maximum applied static pressure load without damage, coinciding with an effort to enhance COLTS capabilities to handle cyclic pressure loading, presented an opportunity for such a testing.

4.1 Efficiency and Control of Pressure Cycling

Low-cycle fatigue pressurization testing of a transport category airframe typically requires tens of thousands of cycles. Thus, the ability to perform such testing in a timely fashion necessitates an automated process for providing rapid pressurization and depressurization capability in a tightly and reliably controlled quasi-static fashion. Primary factors influencing time required per pressure cycle are: (i) supply pressure available, (ii) cyclic pressure level and (iii) volume of the pressurized enclosure. Using the 0.69 MPa (100 psi) pressure supply, target cyclic pressure equal to the DLL of 63.43 kPa (9.2 psi) and for the estimated pressure vessel volume of 2.1 m^3 (74 cu ft.), approximately one cycle per minute was achieved after tuning of the pressure control system in the COLTS facility. Combined with safety measures enabling unmonitored 24-hour operations, this rate translates into approximately 10,000 cycles per week.

The pressure control system operated with a tolerance estimated to be ±0.28 kPa (±0.04 psi). Since the DLL of 63.43 kPa (9.20 psi) was required, to preclude pressure cycles not reaching the nominal value, the control system was set to 63.78 kPa (9.25 psi), i.e., to exceed the nominal value by a small margin in each cycle. Consequently, the nominal DLL pressure was crossed twice within each cycle, i.e., during pressurization and depressurization portion of the cycle. For consistency of the results, the first instance when the pressure would reach the DLL in a cycle was used in post-processing. No cycles truncated below the DLL were identified during testing and the highest recorded over-pressure was 0.8 kPa (0.116 psi), i.e., 1.26% of the nominal DLL.

4.2 Panel Response as a Function of Number of Pressure Cycles

The repaired pressure panel was subjected to the total of 55,000 DLL pressure cycles. Strains measured by the same gages used in the static test were recorded during one full pressure cycle upon completion of 1,000, 10,000, 17,000, 24,000, 31,000, 38,000, 42,000, 45,000 and 55,000 cycles. Strains at the DLL pressure as a function of the number of completed cycles are presented in Figure 15(a)-(c) for the same selected gages discussed in the static test analysis in section 3.3. The same grouping of results as in Figures 12-14 is maintained. Solid lines in Figure 15(a)-(c) correspond to the static test values and dashed lines correspond to the average values obtained from the 10 recordings obtained during the fatigue test cycling. Only small deviations of the cyclic data points from their corresponding averages are seen and there are no appreciable trends observed in the strain responses as the number of cycles was increased that would indicate possible deterioration of structural integrity. However, for nine out of 10 strain measurements considered, the static test produced a larger absolute strain value than the cyclic average. This difference can be explained by a settling process when the initial cycle or a few initial cycles involve some strain hysteresis. This behavior is most evident in the gage shown in blue in Figure 15(c) which was at the tip of the repair flange where the two metallic repair angles were pre-assembled together before being mounted onto the panel. This installation sequence

may have resulted in residual stresses between the two angles being released in the few initial load cycles. Settling trends are also very prominent at two gages in the proximity of single-shear fasteners, shown as blue and red points in Figure 15(b), which can also be a factor promoting the initial settling.

Measured strains as a function of pressure up to the DLL after 1,000 and 55,000 cycles are shown in Figure 15(d) for selected gages on the repair angle and the smooth side of the panel. The data confirms that the pressure-strain curves at the beginning and at the end of the cyclic pressure test match closely indicating no significant changes in the mechanics of the structure.

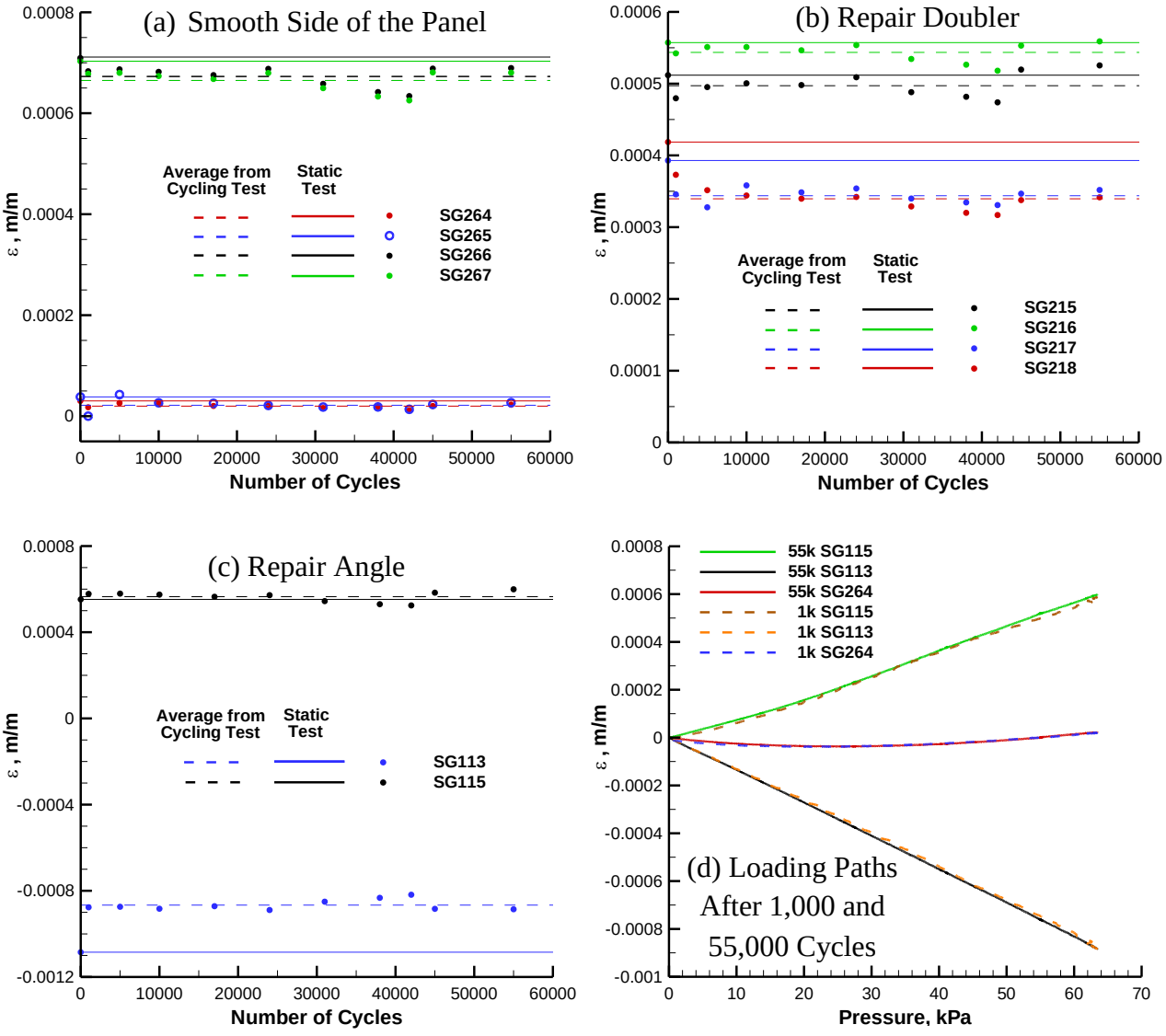

Figure 15. Strains: (a-c) at the DLL pressure as a function of number of cycles, (d) as a function of pressure at 1,000 and 55,000 cycles.

5. CONCLUSIONS

A bolted metallic repair applicable to PRSEUS panels was developed and tested under static tension and pressure loadings. Good correlation with predictive FE analysis supporting the design effort was found. Low-cycle fatigue was also tested and no detrimental effects from 55,000 pressure cycles up to the design limit load were noted. This testing and analysis support upward revision of design allowables for PRSEUS panels which, thus far, were limited by concerns stemming from their repairability. Application of the proposed repair is feasible in the present operational environment using currently available resources.

6. ACKNOWLEDGEMENTS

The authors wish to thank Alex Velicki, Kim Linton and George Mills of the Boeing Company, Research and Technology, Seal Beach, CA for their support of this activity. The FedEx Corporation is gratefully acknowledged for providing personnel from their aircraft maintenance facility at the Los Angeles International Airport to perform repair installation on the pressure panel. A Langley Research Summer Scholar (LaRSS) program participant, R. Travis Kerr, is also recognized for his assistance in performing cyclic pressure test data reduction.

7. REFERENCES

1. Jegley, D. & Velicki, A., "Status of Advanced Stitched Unitized Composite Aircraft Structures." *51st AIAA Aerospace Sciences Meeting*, AIAA-2013-0410, Grapevine, TX, Jan. 2013.

2. Velicki, A. & Jegley, D., "PRSEUS Development for the Hybrid Wing Body Aircraft." *AIAA Centennial of Naval Aviation Forum "100 Years of Achievement and Progress,"* AIAA-2011-7025, Virginia Beach, VA, Sept. 2011.

3. Velicki, A., "Damage Arresting Composites for Shaped Vehicles – Phase I Final Report." NASA/CR-2009-215932, Hampton, VA, Feb. 2009.

4. Velicki, A., Yovanof, N., Baraja, J., Linton, K., Li, V., Hawley, A., Thrash, P., DeCoux, S. & Pickell R., "Damage Arresting Composites for Shaped Vehicles – Phase II Final Report." NASA/CR-2011-216880, Hampton, VA, Jan. 2011.

5. Przekop, A., "Repair Concepts as Design Constraints of a Stiffened Composite PRSEUS Panel." *53rd AIAA/ASME/ASCE/AHS/ASC Structures, Structural Dynamics and Materials Conference*, AIAA-2012-1444, Honolulu, HI, Apr. 2012.

6. Przekop, A. & Jegley, D., "Evaluation of a Metallic Repair on a Rod-Stiffened Composite Panel," *Journal of Aircraft*, in print, DOI: 10.2514/1.C032461.

7. Lovejoy, A., Rouse, M., Linton, K. & Li, V., "Pressure testing of a Minimum Gage PRSEUS Panel." *52nd AIAA/ASME/ASCE/AHS/ASC Structures, Structural Dynamics and Materials Conference*, AIAA-2011-1813, Denver, CO, Apr. 2011.

8. McGowan, D. M., Ambur, D. R. & McNeil, S. R., "Full-field Structural Response of Composite Structures: Analysis and Experiment," *44th AIAA/ASME/ASCE/AHS/ASC Structures, Structural Dynamics and Materials Conference*, AIAA 2003-1623, Norfolk, VA, Apr. 2003.

9. "MSC Nastran 2012.2 Quick Reference Guide." MSC Software Corp., Santa Ana, CA, 2012.

10. Jegley, D., "Experimental Behavior of Fatigue Single Stiffener PRSEUS Specimens." NASA/TM-2009-215955, NASA Langley Research Center, Hampton, VA, Dec. 2009.